THE JOURNAL OF BIOLOGICAL CHEMISTRY VOL. 281, NO. 52, pp. 40164–40173, December 29, 2006

Actinfilin Is a Cul3 Substrate Adaptor, Linking GluR6 Kainate Receptor Subunits to the Ubiquitin-Proteasome Pathway*

Received for publication, August 25, 2006, and in revised form, October 10, 2006 Published, JBC Papers in Press, October 24, 2006, DOI 10.1074/jbc.M608194200

Gregory D. Salinas[‡], Leslie A. C. Blair[‡], Leigh A. Needleman[‡], Justina D. Gonzales[§], Ying Chen[¶], Min Li[¶], Jeffrey D. Singer[§], and John Marshall[‡1]

From the Departments of [‡]Molecular Pharmacology, Physiology, and Biotechnology and [§]Molecular Biology, Cell Biology, and Biochemistry, Brown University, Providence, Rhode Island 02912 and the [¶]Department of Neuroscience, Johns Hopkins University, School of Medicine, Baltimore, Maryland 21205

Kainate receptors have been implicated in excitotoxic neuronal death induced by diseases such as epilepsy and stroke. Actinfilin, a synaptic member of the BTB-Kelch protein family, is known to bind to the actin cytoskeleton. However, little is understood about its function at the synapse. Here, we report that actinfilin is able to bind to GluR6, a kainate-type glutamate receptor subunit, and target GluR6 for degradation. Like many members of its protein family, actinfilin acts as a substrate adaptor, binding Cullin 3 (Cul3) and linking GluR6 to the E3 ubiquitin-ligase complex. We map this interaction to the Kelch repeat domain of actinfilin and the GluR6 C terminus. Co-immunoprecipitation and immunofluorescence studies show that GluR6 is ubiquitinated, and that GluR6 levels are decreased by actinfilin overexpression but increased when actinfilin levels are reduced by specific RNA interference. Furthermore, actinfilin-Cul3 interactions appear to be important for regulating surface GluR6 expression. Synaptic GluR6 levels are elevated in mice with lowered neuronal Cul3 expression and when dominant-negative forms of Cul3 are transfected into hippocampal neurons. Together our data demonstrate that actinfilin acts as a scaffold, linking GluR6 to the Cul3 ubiquitin ligase to provide a novel mechanism for kainate receptor degradation.

Ionotropic glutamate receptors mediate fast excitatory neurotransmission in the mammalian brain and, based on agonist sensitivity, are subdivided into the *N*-methyl-D-aspartic acid (NMDA),[2] α-amino-3-hydroxy-5-methylisoxazole-4-propionic acid (AMPA), and kainate receptor families. Kainate receptors (KARs) consist of tetrameric assembly of five subunits, GluR5–7 and KA1–2, to control intrinsic excitability, regulate transmitter release and are implicated in epileptiform activity (1, 2). GluR5–7 can form functional homomeric or heteromeric receptors, whereas KA1 and KA2 assembly with GluR5–7 subunits is necessary for their intracellular trafficking and formation of functional receptors (3–6). We and others have shown that the cytoplasmic C-terminal region of KAR subunits contain trafficking signals and bind a number of PDZ domain-containing proteins, such as PSD-95 (5, 7–11). Presynaptically, KARs modulate transmitter release at both excitatory and inhibitory synapses and may be involved in long-term synaptic plasticity via PDZ domain interactions (1, 2). In hippocampal neurons, postsynaptic GluR6-containing KARs mediate a slow excitatory synaptic current (6, 12–15), and can also enhance excitability through a metabotropic inhibition of a calcium-activated potassium channel (I_{sAHP}) via G-protein and protein kinase C activation (6, 16–18). Using KAR knock-out mice the metabotropic inhibition of I_{sAHP} was found to be dependent on the KA2 subunit, which interacts with $G_{q/11}$ proteins known to be involved in this modulation (6).

KAR degradation is known to involve activity-dependent endocytosis, in which GluR6-containing receptors are sorted for recycling or degradation (19). Ubiquitination plays an important role in regulating the abundance of many synaptic proteins and destabilizing receptors within the postsynaptic density (20–22). The selection of substrates for ubiquitination is accomplished by an E3 ligase that consists of a complex of proteins that act together to transfer ubiquitin to the substrate at specific lysine residues. This results in the attachment of a polyubiquitin tag that targets the substrate for proteasomal degradation (23). Two major families of E3 ligases have been described: the HECT domain family and the RING family, which includes the closely related Cullin proteins, Cul1 and Cul3 (23). Cullin-based E3 ligases function as large protein complexes. One of the best characterized is the Skp1-Cul1-F box-Roc1 complex, in which Cul1 binds an adaptor molecule, Skp1, via an N-terminal domain, and a small RING finger protein, RBX1/Roc1, via a C-terminal domain (23). Through Skp1, Cul1 associates with an F-box protein that in turn binds a phosphorylated substrate to target it for degradation.

Recent studies show that Cul3 associates with substrate-specific adaptors consisting of an N-terminal BTB motif (from bric a brac, tramtrack, and broad complex) and a series of C-terminal Kelch repeats (24, 25). Actinfilin, an actin-binding protein of unknown cellular function, contains a BTB domain, six Kelch domain repeats, and a C-terminal PDZ binding motif (26, 27). Using a yeast

* This work was supported by National Institutes of Health Grants RO1 NS39063 and NS39309 and the DEARS Foundation (to J. M), the Emerald Foundation and COBRE (to J. D. S), and National Institutes of Health Grant GM070959 (to M. L.). The costs of publication of this article were defrayed in part by the payment of page charges. This article must therefore be hereby marked "*advertisement*" in accordance with 18 U.S.C. Section 1734 solely to indicate this fact.

[1] To whom correspondence should be addressed. Tel.: 401- 863-2574; Fax: 401-863-1595; E-mail: John_Marshall@brown.edu.

[2] The abbreviations used are: NMDA, *N*-methyl-D-aspartic acid; KAR, kainate receptors; TRITC, tetramethylrhodamine isothiocyanate; RNAi, RNA interference; GFP, green fluorescent protein; HA, hemagglutinin; CHAPS, 3-[(3-cholamidopropyl)dimethylammonio]-1-propanesulfonic acid; SM, starting material; AF, actinfilin.

two-hybrid screen with the GluR6 C terminus as bait, we identified actinfilin as a potential binding partner. Here, we show that actinfilin specifically binds GluR6 and mediates its degradation via the ubiquitin-proteasome pathway.

EXPERIMENTAL PROCEDURES

Antibodies—The monoclonal anti-myc (9E10), anti-GFP (B2), and anti-SAP97 (hDlg) antibodies were purchased from Santa Cruz (Santa Cruz, CA) and used at 1:200 for immunoblotting. The monoclonal anti-PSD-95, polyclonal anti-GluR6/7 (1:500 for immunoblotting), polyclonal anti-KA2, polyclonal anti-GluR5, polyclonal anti-NR2B, and mouse anti-Kv1.4 antibodies were from Upstate (Waltham, MA). The mouse anti-GluR2 and mouse anti-actin (1:5,000 for immunoblotting) antibodies were from Chemicon (Temecula, CA). The monoclonal anti-FLAG antibody was from Sigma. The monoclonal anti-NR1 antibody was from BD Biosciences. The monoclonal anti-HA antibody was from obtained from Covance (Princeton, NJ) and used at 1:1000. The rabbit anti-GluR6 antibody was generated using as an antigen a peptide (C-GAQDDVNGQWWG) that was predicted, from crystallographic analyses, to form part of an exposed extracellular loop in the GluR6 S1 domain; the antibody was affinity purified and used at 1:50–1:200. The rabbit anti-actinfilin antibody (1:5000 for immunoblotting) is described in Ref. 26. The rabbit anti-Cul3 antibody was developed as previously described (40) and used at 1:500 for immunoblotting. For heterologous cell and neuronal immunostaining, mouse anti-AFP (1:500) was from Q-Biogene (Irvine, CA). The goat anti-myc antibody was from Santa Cruz. The fluorescent secondary antibodies were purchased from Jackson ImmunoResearch (West Grove, PA).

Yeast Two-hybrid—The Matchmaker yeast protocol (Clontech) was followed for proper transformation of plasmid DNA in the AH109 strain of yeast, made chemically competent with the lithium acetate method. The C terminus of GluR6 was subcloned into the pGBKT7 bait vector from amino acid 852-stop, fused to the GAL4 DNA-binding domain. GluR6-Cterm/pGBKT7 transformants were selected on tryptophan-deficient (Trp−) medium and subsequently transformed with an oligo(dT)-primed hippocampal cDNA library subcloned into pGADT7. For medium stringency conditions, positive clones were selected on triple-deficient plates (His-, Leu-, and Trp-), and viable colonies then streaked onto higher stringency media plates (-Ade-Leu-His-Trp/X-α-galactosidase), and selected for growth and blue colonies. Plasmid DNA was isolated using the RPM Yeast Plasmid isolation kit (Bio 101, Vista, CA) and transformed into Top 10F′ *Escherichia coli* (Invitrogen). The complete rat actinfilin cDNA and truncations were subcloned into the pGADT7 prey vector. Two actinfilin truncations were subcloned from amino acids 1–344 and 279-stop. The relative levels of interaction with the GluR6 C terminus were assessed by determining the levels of dropout in selective media of increasing stringency.

Molecular Biology of GluR6 Truncations and Mutations—*GFP-GluR6* was obtained from Dr. Steve Heinemann (The Salk Institute for Biological Studies, La Jolla, CA); GFP was inserted after the signal sequence of pcDNA3-*pGluR6*(*Q*). The *myc*-tagged *actinfilin* and its two truncations are described in Ref. 26. nAchRγ-HA was received from Dr. Edward Hawrot (Brown University, Providence, RI). The HA-tagged GABA-B-R1 and -R2 constructs were gifts from Dr. Steve Moss (University of Pennsylvania, Philadelphia, PA). The eight full-length *GluR6* constructs with progressively generated stop codons (*GFP-GluR6–850*, *-854*, *-868*, *-874*, *-880*, *-887*, *-896*, and *-904*) were gifts from Dr. Geoffrey Swanson (Northwestern University, Chicago, IL). The yeast two-hybrid constructs were produced by PCR amplification, digested with EcoRI and BamHI restriction enzymes, and ligated into the vectors PGBKT7 and pGADT7 (Clontech). Alanine scanning of the *GFP-GluR6–887* construct was performed using the QuikChange site-directed mutagenesis protocol (Stratagene). All constructs were verified by DNA sequencing prior to transfection.

Rat Cerebellar Extracts—Three cerebelli from adult Sprague-Dawley rats were dissected and placed in 10 ml of cold phosphate-buffered saline. The tissue was mechanically homogenized with a Tissuemizer and spun at 1000 × *g* to pellet debris. The pellet was then solubilized in an equal amount of 0.6% CHAPS buffer (150 mM NaCl, 20 mM HEPES, pH 7.4, 2 mM EDTA, 5% glycerol, 0.6% CHAPS + protease inhibitors (1 mM benzamidine, 1 mM phenylmethylsulfonyl fluoride, and a protease inhibitor mixture containing 2.08 mM 4-(2-aminoethyl)benzenesulfonyl fluoride, 1.6 μM aprotinin, 0.04 mM leupeptin, 0.08 mM bestatin, 0.03 mM pepstatin A, 0.028 mM E-64)) by pulling through syringe needles of decreasing size. The solute was spun at 39,000 × *g* for 30 min and the supernatant removed as the final extract.

Cell Culture and Transfection—HEK293 and COS7 cells (ATCC, Manassas, VA) were plated onto 60-mm cell culture dishes, and grown to 70% confluency in Dulbecco's modified Eagle's media (high glucose with L-glutamine) (Invitrogen) with 10% fetal bovine serum (Gemini Bioproducts) and a 1% penicillin (10,000 units/ml) and streptomycin (10 mg/ml) mixture (Sigma). Hippocampal neurons were cultured from E18 rats and maintained in Neurobasal medium supplemented with B27 and Glutamax (28). For immunocytochemistry experiments, cells were plated onto 0.1 mg/ml poly-D-lysine-coated glass coverslips. HEK293 cell transfections were performed with FuGENE 6 transfection reagent (Roche) following the manufacturer's protocol for transient transfection of adhered cells. Hippocampal neurons and COS7 cells were transfected with Lipofectamine 2000 reagent (Invitrogen), following the manufacturer's recommended protocol. For conditions including MG132 (Calbiochem) or leupeptin (U. S. Biochemical Corp.), cells were incubated with the drugs for 4 h prior to fixation or solubilization unless stated otherwise.

HEK293 Extracts, Co-immunoprecipitations, and Western Blots—48 h after transfection, cells were washed once with cold Tris-buffered saline and harvested in 1 ml of 0.6% CHAPS buffer + protease inhibitors (as indicated above). The cells were homogenized by pipetting and rotated at 4 °C for 1 h to complete solubilization. Extracts were then centrifuged at 14,000 × *g* for 30 min to pellet debris, removing the supernatant for immunoprecipitations and immunoblotting. For co-immunoprecipitation, extracts were incubated with 4 μg of each antibody at 4 °C overnight. The solution was then incubated with 50 μl of 50% protein G-Sepharose/Tris-buffered saline slurry for

1 h at 4 °C. The beads were washed three times with 0.6% CHAPS buffer, and bound proteins were eluted by boiling in sample buffer. Samples were separated by 8 or 12% SDS-PAGE, electrotransferred, and immunostained. Expression levels in the total cell extracts (starting material, SM) were established by Western blot analyses. Protein bands were visualized using Super-signal West Pico chemiluminescent substrate (Pierce). Band intensities were analyzed using Image J software (NIH), and graphs were developed with SigmaPlot 8.0 (Systat Software).

Immunofluorescence—24–48 h after transfection, cells were fixed with 1.5% paraformaldehyde + 3% sucrose, washed, permeabilized with 0.01% Triton X-100, and nonspecific binding sites blocked with 4% goat or donkey serum (depending on the source of the secondary antibody). For detection of surface epitopes, the permeabilization step was omitted; for detecting both surface and intracellular epitopes, sequential labeling was employed. Briefly, cells were incubated overnight at 4 °C with the relevant primary antibody, washed to remove unbound primary antibody, and exposed to Cy5-, TRITC-, or fluorescein isothiocyanate-conjugated secondary antibodies (Jackson Immunoresearch Laboratories). Labeling was visualized under fluorescence optics using a Zeiss Axiovert 200M fluorescence microscope or a Leica TCS SP2 AOBS scanning laser confocal microscope. The sizes of GluR6 puncta and their percent colocalization of GluR6 with YFP-PSD-95 or synaptophysin was determined using Image J analysis software (NIH).

Cul3 Heterozygous Knock-out Mice and Synaptosome Preparation—Mice heterozygous for the *Cul3* gene were as described in Singer *et al.* (29). P14 mouse brains were dissected, weighed, equalized, and homogenized in a buffer containing 0.32 M sucrose and 4 mM HEPES, pH 7.4. This solution was centrifuged at 1,000 × *g* at 4 °C for 5 min. Another 500 μl of buffer was added to this pellet, which was again homogenized and centrifuged. The supernatant was taken, and an aliquot was removed for a whole cell brain fraction extract. The remaining supernatant was centrifuged at 10,000 × *g* to pellet a crude synaptosomal fraction. For analysis, 10 μl of the whole cell extract was combined with 10 μl of sample buffer. The synaptosome pellet was solubilized in 200 μl of sample buffer, then resolved via 8 or 12% SDS-PAGE and immunoblotted.

GST Pulldowns of Polyubiquitinated Proteins—To assess GluR6 ubiquination in brain tissue, crude synaptosomes of wild-type (*Cul3*$^{+/+}$) and heterozygous *Cul3*$^{+/-}$ P14 mice were solubilized and denatured in Tris-buffered saline containing 0.2% SDS at 70 °C for 10 min, then diluted into 1% Triton X-100 and 5% glycerol. To prevent deubiquitination in solution, samples were kept in 1 μM ubiquitin aldehyde and 50 μM MG132 throughout. GST-S5a beads (Biomol, Exeter, United Kingdom), which are composed of the proteasomal subunit S5a conjugated with agarose, or GST-agarose beads were added to the sample for 2 h at 4 °C. The S5a beads are designed to bind ubiquitinated substrates *in vitro*. The beads were washed with Tris-buffered saline + 1% Triton X-100 + 5% glycerol and eluted by boiling in SDS-PAGE loading buffer. Equal levels of GluR6 were resolved by SDS-PAGE, transferred to nitrocellulose, and immunoblotted for the presence of ubiquitin.

RESULTS

Actinfilin Binds GluR6—Using the GluR6 C terminus as bait for a yeast two-hybrid screen, we identified several cDNA clones fragments whose open reading frames encode the BTB/Kelch domain protein, actinfilin. Actinfilin (AF) was previously shown to be largely localized to the brain, especially in the cerebrum and cerebellum and is present in the postsynaptic density (26). The AF protein contains a proline-rich N terminus, followed by a POZ/BTB domain, a BACK domain, six Kelch domain repeats, and a C-terminal PDZ binding motif. Recent evidence suggests that the role of several BTB domain-containing proteins is related to protein degradation, involving Cul3 and the E3 ubiquitin-ligase pathway (24, 25). The localization of actinfilin in postsynaptic areas of the cerebellum suggested that actinfilin may be involved in the degradation of key proteins involved in neuronal transmission. To assess specificity and determine whether the interaction between actinfilin and GluR6 could be detected in brain we performed a co-immunoprecipitation assay (Fig. 1*A*, *top panel*). We found that actinfilin specifically binds GluR6 and GluR5 in the rat cerebellum, but does not interact with the potassium channel Kv1.4, AMPA receptor subunit GluR2, or the NMDA receptor subunits NR1 and NR2B. Controls indicate specificity that actinfilin does not recognize proteins immunoprecipitated by a nonspecific rabbit antibody (IgG) or proteins pulled down solely by Protein G-Sepharose beads without added antibody (beads alone). To characterize its specificity further, we carried out additional coimmunoprecipitation assays of transiently cotransfected plasmids expressing myc-tagged actinfilin with several postsynaptic receptors and scaffolding proteins in HEK293 cells. As shown in Fig. 1*A* (*lower panel*), actinfilin binds to GFP-tagged GluR6 and GFP-GluR5, but not to GFP-GluR1, HA-tagged nAchRγ, KA2, PSD-95/SAP90, SAP97, HA-GABA-B-R1, and HA-GABA-B-R2.

Actinfilin Truncation Analysis—To determine the region of actinfilin responsible for the binding to GluR6, we utilized the yeast two-hybrid binding system. Actinfilin or one of the two truncations (Fig. 1*B*) fused to the yeast activation domain were co-transformed with the C terminus of the GluR6/GAL4 DNA-binding domain bait plasmid (Fig. 1*B*). We observed that actinfilin and the Kelch repeats bound the GluR6 C terminus, but the BTB/POZ domain failed to interact. However, full-length actinfilin gave many more transformants than the Kelch region alone on high stringency media, suggesting that it exhibits a higher affinity interaction. The binding data were confirmed by coimmunoprecipitation using myc-tagged truncation constructs identical to the yeast two-hybrid constructs (37). These experiments confirmed that the Kelch truncation is able to bind full-length GluR6, whereas the BTB/POZ truncation cannot (Fig. 1*C*).

Actinfilin and Cul3 Interact—If actinfilin is a member of the BTB/POZ-Kelch protein family involved in protein degradation, it might be predicted to bind Cul3, the scaffold for the Cul3-based E3 ubiquitin-ligase complex (30–32). In co-immunoprecipitation experiments, myc-tagged actinfilin pulled down FLAG-tagged Cul3 (Fig. 2*A*). A mutant Cul3 (L52A/E55A) (33), designed to prevent interaction with BTB proteins

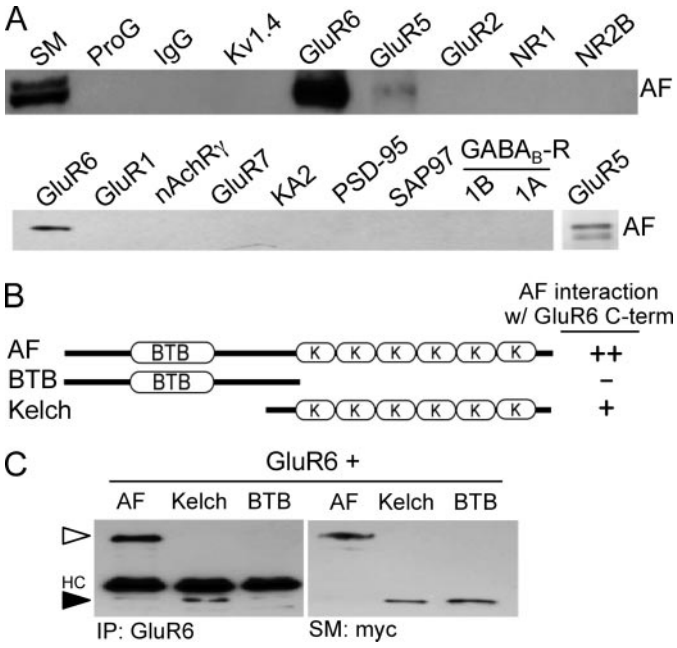

FIGURE 1. **Actinfilin specifically binds GluR6 through its Kelch repeats.** *A*, actinfilin (*AF*) interacts strongly with GluR6. *Top panel*, rat cerebellar extracts: glutamate receptor subunits (GluR6, GluR5, GluR2, NR1, NR2B) and an ion channel (Kv1.4) were individually immunoprecipitated (*IP*), then immunoblotted for the presence of AF. GluR6, and to a lesser degree GluR5, were found to bind. Controls, shown in the *first three lanes*, demonstrate that nonspecific binding of the AF antibody is low, and include total cerebellar AF levels (*SM*), Protein G beads alone (*ProG*), and nonspecific rabbit IgG. *Bottom panel*, HEK293 cells transfected with myc-tagged AF. Individual receptor subunits or scaffolding proteins were individually immunoprecipitated using antibodies specific for each protein or an epitope tag; GluR1, -5, and -6 were GFP-tagged, nAchRγ and GABA$_B$ receptors were HA-tagged, GluR7, KA2, and PSD-95 were immunoprecipitated using specific antibodies against each protein. Immunoprecipitates were then immunoblotted for the myc epitope to detect AF; GluR6 and GluR5 interact with AF. No binding was observed with the AMPA receptor subunit GluR1, nAchRγ subunit, the kainate receptor subunits GluR7 or KA2, scaffold proteins PSD-95 and SAP97, or GABA-B-R1 or -R2 receptors. *B*, full-length AF, AF truncations, and their relative levels of interaction with the GluR6 C terminus as assessed via a yeast two-hybrid assay. Both the full-length AF and the Kelch domain construct interact with the GluR6 C terminus. No interaction with the BTB domain was detected: − indicates that no colonies were obtained in medium stringency conditions; + indicates that growth was obtained in medium stringency conditions, but that few colonies were obtained at high stringency; and ++ indicates that numerous colonies grew in high stringency conditions (see "Experimental Procedures"). *C*, *left panel*, full-length GluR6 interacts with both full-length AF (*open arrowhead*) and the Kelch domains (*solid arrowhead*). GFP-tagged GluR6 was transfected into HEK293 cells with full-length myc-tagged AF, myc-tagged-Kelch, or myc-tagged-BTB. GluR6 was immunoprecipitated via the GFP epitope and co-precipitants were identified by immunoblotting for the myc tag. The position of the antibody heavy chain is also indicated (*HC*). *Right panel*, starting material extracts (*SM*), resolved via SDS-PAGE and immunoprobed for the presence of the myc tag, demonstrate that the BTB domain construct expresses as well as the Kelch domain construct. Note that the Kelch and BTB truncations run at similar positions.

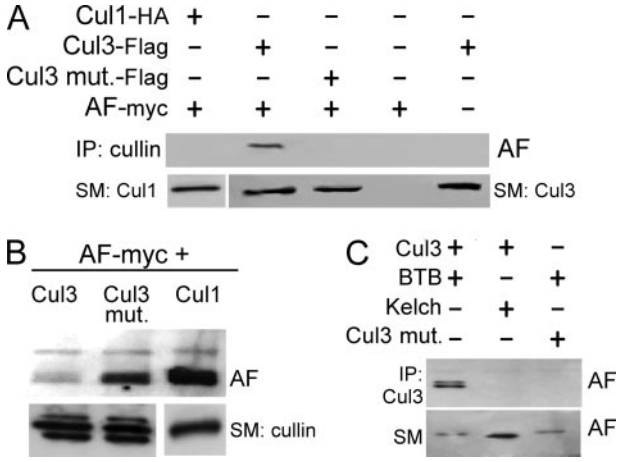

FIGURE 2. **Actinfilin binds Cul3 through the BTB domain.** *A*, AF co-immunoprecipitates (*IP*) with wild-type Cul3 (*lane 2*), but not with Cul1 (*lane 1*) or mutant L52A/E55A Cul3 (*lane 3*) in transfected HEK293 cells. Controls, shown in *lanes 4* and *5*, demonstrate the absence of co-immunoprecipitation when cells are transfected with AF alone or Cul3 alone. The *lower panel* shows Cullin expression levels in SM extracts. Blots were probed for HA-tagged Cul1 (*lane 1*) or FLAG-tagged Cul3 (*lanes 2–5*). *B*, Cul3 down-regulates AF levels. HEK293 cells were co-transfected with myc-AF and Cullin constructs and total cell extracts were immunoblotted for the presence of AF. Cul3 (−*Flag-tagged*) strongly reduces AF expression. In the presence of Cul3-FLAG L52A/E55A or Cul1-HA, AF expression is considerably higher. *Lower blots*, all three Cullin constructs expressed well. Blots of SM extracts were probed for FLAG-tagged Cul3 (*lanes 1* and *2*) or HA-tagged Cul1 (*lane 3*). *C*, Cul3 interacts with AF via the AF BTB domain. When HEK293 cells were co-transfected with FLAG-tagged wild-type Cul3 and myc-tagged AF truncation constructs, the BTB domain co-immunoprecipitated with Cul3 (*lane 1*), but the Kelch domain did not (*lane 2*). However, the BTB domain failed to co-precipitate with the L52A/E55A mutant Cul3-FLAG (*lane 3*). The *lower panel* demonstrates that AF constructs are present in all SM extracts.

was unable to bind actinfilin (Fig. 2*A*). Additionally, a similar Cullin, Cul1, was also unable to bind actinfilin. Significantly, when actinfilin is coexpressed with wild-type Cul3, its expression is substantially lowered, whereas neither the mutant L52A/E55A Cul3 nor Cul1 exerted any substantial effect on actinfilin levels (Fig. 2*B*). This suggests that the Cul3 ubiquitin-ligase complex may also affect the adaptor protein actinfilin as well as the substrate. The actinfilin-Cul3 interaction, as expected for this protein family, occurs within the BTB/POZ domain. The FLAG-Cul3 immunoprecipitated the myc-tagged BTB/POZ actinfilin truncation, whereas the Kelch truncation (lacking the BTB domain) did not (Fig. 2*C*).

Actinfilin Promotes GluR6 Degradation—To examine the effects of actinfilin on GluR6 abundance, localization, or sequestration in organelles, we co-transfected actinfilin and GFP-GluR6 into COS-7 cells. When expressed alone, GFP-GluR6 exhibited a punctate staining throughout the cell. However, upon introducing myc-tagged actinfilin, immunostaining for GluR6 was abrogated (Fig. 3*A*), suggesting that actinfilin promotes degradation of this kainate receptor subunit. This hypothesis was confirmed immunocytochemically by the use of proteasomal inhibitors and by co-expression of dominant-negative constructs to shift the equilibrium away from GluR6 degradation (Fig. 3*A*). The hypothesis was further substantiated by immunoblotting for total GluR6 levels (Fig. 3*C*). We found that the GFP-GluR6 signal is restored by treatment with the proteasomal inhibitor MG132 (25 μM) for 4 h prior to fixation (Fig. 3, *A*, *third panel*, and *C*, *lane 4*). The lysosomal inhibitor leupeptin (10 μg/ml, 4 h incubation) exerted a weaker effect (Fig. 3, *A*, *fourth panel*, and *C*, *lane 5*), suggesting that actinfilin promotes degradation primarily through proteasomal pathways. Consistent with these pharmacological results, we found that co-expression of the Cul3 mutant L52A/E55A that prevents interaction with BTB proteins, but not wild-type Cul3, blocked GluR6 degradation (Fig. 3, *A*, *fifth versus sixth panels*, and *C*, *lane 6*). Similarly, co-expression of HA-tagged ubiquitin K48R, which prevents the attachment of Lys^{48} branched ubiquitin chains, partially elevated GluR6 levels (Fig. 3, *A*, *seventh panel*, and *C*,

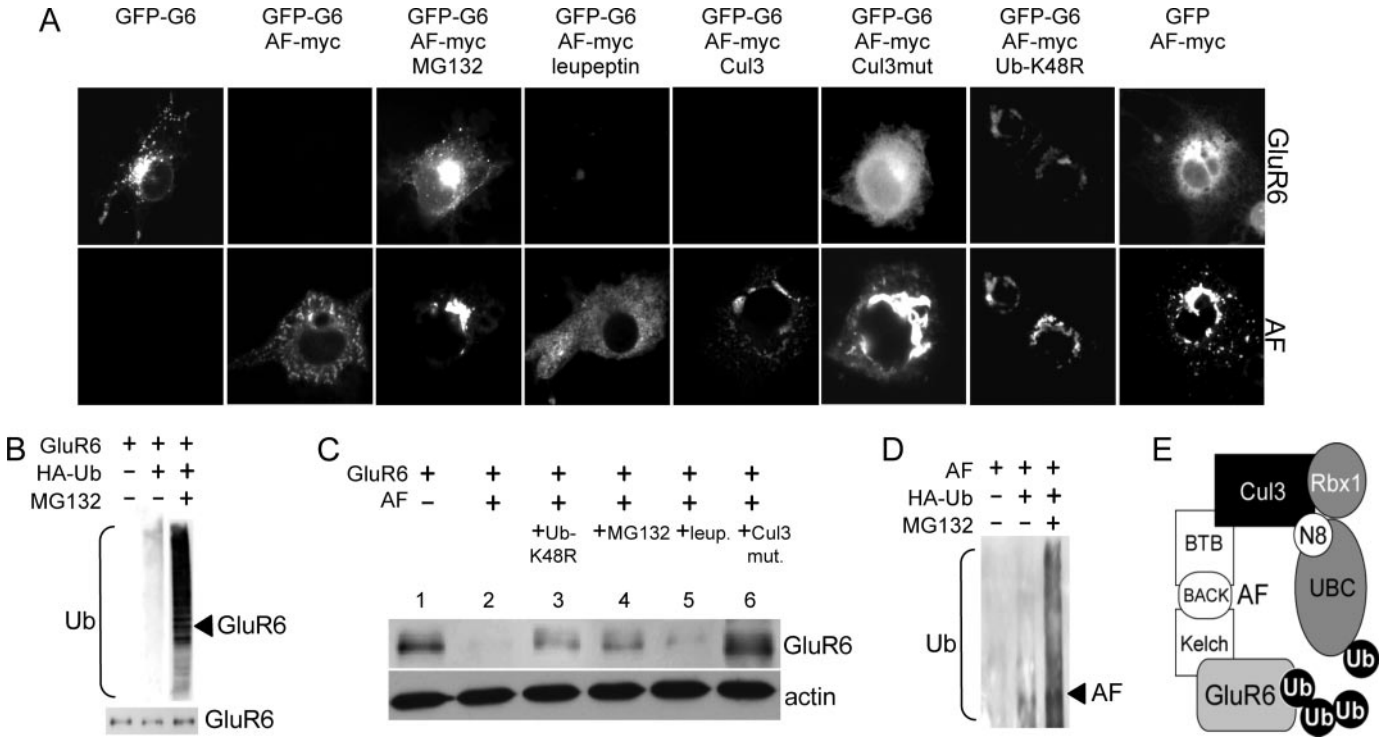

FIGURE 3. **Actinfilin mediates GluR6 degradation primarily through proteasomes.** *A*, actinfilin-mediated degradation of GluR6 is largely blocked by proteosomal inhibitors or by co-expression with mutant Cul3 or a ubiquitin (*Ub*) construct that prevents polyubiquination. COS7 cells were transfected as indicated. Cells were permeabilized and stained with antibodies against the GFP tag to reveal total GluR6 labeling (*top row*) and with antibodies to the myc tag to reveal total AF labeling (*bottom row*). Expressed alone, GluR6 staining (*GFP-G6*) is both diffuse and punctate. Co-expression with myc-AF causes total loss of GluR6 signal. This signal is recovered with addition of the proteasomal inhibitor MG132 (25 μM) 4 h prior to fixation and by co-transfection with L52A/E55A Cul3-FLAG or ubiquitin-K48R, a mutant form of ubiquitin that blocks some ubiquitin-mediated degradation by preventing Lys^{48} branched polyubiquination. In contrast, lysosomal inhibition (10 μg/ml leupeptin, 4 h) does not restore the GluR6 signal. Similarly, GluR6 levels are low in the presence of wild-type Cul3. As a control to ensure that AF was not targeting GFP for degradation, GFP levels were also assessed in cells co-transfected with AF and GFP (*far right*). *B*, GluR6 can be ubiquitinated *in vitro*. HEK293 cells were transfected with GFP-GluR6 with or without HA-tagged ubiquitin, GluR6 immunoprecipitated, and precipitates immunoblotted for the presence of the HA epitope. When ubiquitin and GluR6 are co-expressed, they co-immunoprecipitate, with the GluR6 appearing as a smear typical of polyubiquitin-mediated degradation. Blocking proteasomal degradation by incubation in MG132 (25 μM) for 4 h prior to solubilization greatly enhances detectable GluR6 ubiquitination. The *arrowhead* designates the approximate molecular weight for GluR6. Total levels of GluR6 are shown *below*. *C*, actinfilin degrades GluR6 in a Cul3-, ubiquitin- and proteasome-dependent manner. Western blot analyses confirms the immunocytochemical results, demonstrating that AF decreases GluR6 expression (*lanes 1 versus 2*). Equal amounts of total cell extracts were resolved via SDS-PAGE, and Western blots were probed for the presence of the receptor (*upper panel*). A ubiquitin mutant that prevents polyubiquitin chains (Ub-K48R) and proteasomal inhibition (25 μM MG132) partially restore GluR6 expression (*lanes 3* and *4*), whereas lysosomal inhibition (10 μg/ml leupeptin) has relatively little effect (*lane 5*). L52A/E55A Cul3, which acts as a dominant-negative, enhances GluR6 expression by restricting the ability of AF to bind to Cul3 (*lane 6*). As a control to ensure that equal amounts of cell extracts were used, blots were also probed for actin (*lower panel*). *D*, actinfilin is also polyubiquitinated. AF-myc and ubiquitin-HA co-immunoprecipitate from transfected HEK293 cells (*lane 2*) and, when proteasomal degradation is inhibited with 25 μM MG132, the level increases. *E*, a model of how actinfilin links GluR6 to Cul3 and the E3 ubiquitin-ligase complex: Cul3 is a component of an E3 ubiquitin-ligase complex, also composed of the proteins Nedd8 (*N8*), Rbx1, and a ubiquitin-conjugating enzyme (*UBC*). AF acts as an adaptor to link GluR6 to this complex, binding GluR6 through the Kelch domain and Cul3 through the BTB domain, and enabling ubiquitination of the receptor subunit.

lane 3). As a control, we tested if actinfilin affected the expression of the GFP; none was observed (Fig. 3*A*, *eighth panel*).

GluR6 Is Ubiquitinated in Vitro—To determine whether GluR6 is ubiquitinated in cell culture, we co-transfected a myc-tagged GluR6 construct with an HA-tagged ubiquitin, immunoprecipitated the GluR6, and immunoprobed for the HA signal. The level of ubiquitinated GluR6 was low (Fig. 3B). However, treatment with the proteasomal inhibitor, MG132 (25 μM), for 4 h prior to extraction greatly enhanced the amount of ubiquitinated GluR6 in the cells (Fig. 3*B*). Interestingly, actinfilin can also be ubiquitinated (Fig. 3*D*). Based on all preceding data, we hypothesize that actinfilin is acting as an intermediary between GluR6 and Cul3, enabling the ubiquitination of GluR6 (Fig. 3*E*).

Truncation and Mutational Analysis of the Actinfilin-GluR6 Interaction—To identify region(s) on GluR6 that are required for the actinfilin interaction, we utilized a series of C-terminal deletion constructs (Fig. 4*A*). Co-transfecting GluR6 truncations with myc-actinfilin in HEK293 cells suggested that only the GFP-G6–887 truncation and the full-length constructs can bind actinfilin (Fig. 4*B*). We conclude that a region encompassing amino acids 881–886, containing a unique hydrophobic sequence APVIV is critical for GluR6-actinfilin binding. It should be noted that total levels of these truncation constructs correspond with the amount of actinfilin binding, as both the GFP-G6–887 and full-length GluR6 exhibited lower total expression than the other truncation constructs. Thus, binding of actinfilin leads to receptor degradation. Immunocytochemical analyses confirmed these results (Fig. 4*C*).

To map the residue(s) in the hydrophobic region that influence actinfilin binding, we performed alanine-scanning mutagenesis in the GFP-GluR6–887 construct, which was more resistant to degradation (Fig. 5*A*). Expression of the constructs varied (Fig. 5*B*, *top panel*); therefore, to determine the

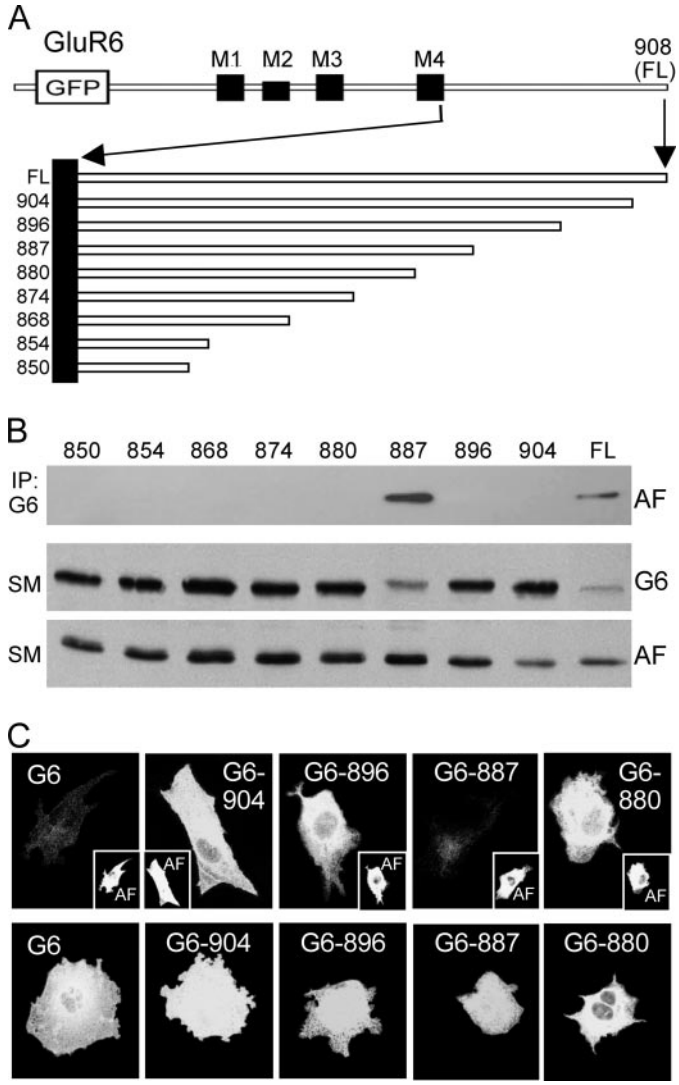

FIGURE 4. **C-terminal truncations of GluR6: manipulation of actinfilin binding.** *A*, schematic of GFP-tagged GluR6 constructs in which progressively more C-terminal residues have been removed. Full-length GluR6 (*FL*) terminates at amino acid 908; *numbers* at the *left* indicate the amino acid position in each truncation construct that was mutated to a stop codon. Known membrane-associated sequences (*M1–M4*) are also shown. *B*, only the full-length GFP-G6 and the GFP-G6 – 887 constructs bind AF. Full-length and GluR6 C-terminal truncation constructs were co-expressed with AF-myc in HEK293 cells, and the GluR6 immunoprecipitated (*IP*) using an anti-GFP antibody. The *upper blot* was probed for the presence of AF using antibodies against the myc tag. *Middle* and *lower blots* show the total levels (*SM*) of the GFP-GluR6 (*G6*) and AF-myc constructs. Note that little full-length or 887-truncation GluR6 is detected, presumably due to AF-induced degradation, whereas the total GluR6 levels are high for the truncations that fail to interact with AF. Note also that full-length GluR6 is more efficiently degraded than the GluR6 – 887; the lower amount of detectable co-immunoprecipitate seen in the *upper panel* is most likely due to more efficient degradation of the full-length construct. *C*, actinfilin reduces the expression of full-length GluR6 and the GluR6 – 887 C-terminal truncation. *Upper panels*, GluR6 levels (*G6*), revealed via the GFP epitope, in COS7 cells co-transfected with AF-myc and full-length GFP-G6 (*far left*) or the indicated GFP-tagged truncation constructs. *Insets* show AF labeling in the same cells and demonstrate that AF expressed well. *Lower panels*, GluR6 levels in COS7 cells transfected only with the GFP-G6 constructs reveal that all constructs express well, indicating that the low GluR6 and the GluR6 – 887 observed in the presence of AF was specific to the AF.

relative levels of binding, we equalized receptor levels for the starting protein extracts in the co-immunoprecipitation analyses (Fig. 5*B*, *middle panel*). As would be predicted from the observation that actinfilin strongly reduced GluR6 levels (Fig. 3), we found that mutants with higher overall expression levels (V883A and I884A) exhibited no interaction with actinfilin (Fig. 5*B*, *lower panel*). Immunostaining substantiates these results. The V883A and I884A mutations protect these GluR6 constructs from the actinfilin-mediated degradation seen with the wild-type GFP-G6 – 887 construct (Fig. 5*C*).

If actinfilin acts as an adaptor to link GluR6 to the ubiquitin-proteasome pathway, then actinfilin would be expected to increase the ubiquitination of GluR6. To examine the effect of actinfilin on GluR6 ubiquitination, we co-transfected wild-type or Ile^{884} mutated full-length GFP-GluR6 with and without HA-tagged ubiquitin-K48R and myc-tagged actinfilin in HEK293 cells. To block signal loss due to proteasomal degradation, 10 μM MG132 was added 10 h prior to solubilization. Cell extracts were immunoprecipitated with antibodies against GFP, and immunoblotted for the presence of HA ubiquitination. We found that ubiquitination of wild-type GluR6 increases in the presence of actinfilin, but as expected for the GluR6 I884A mutant that does not bind actinfilin, there is no difference in the ubiquitination of GluR6 I884A with or without actinfilin (Fig. 5*D*).

Decreased Neuronal Cul3 Levels Increase Synaptic, Ubiquitinated GluR6—To determine whether GluR6 is regulated in the Cul3-mediated pathway, we utilized a mouse strain with reduced Cul3 expression levels (29). Because homozygous *Cul3* knock-out mice are embryonic lethal, we used heterozygous knock-out mice, which have 50% decreased Cul3 expression in the brain (Fig. 6*A*), but otherwise develop normally.[3] Crude synaptosomes were prepared from heterozygous $Cul3^{+/-}$ and wild-type mice, and equal amounts were resolved via SDS-PAGE to observe comparative changes in expression (Fig. 6*B*); GluR6 levels are increased in heterozygous brain synaptosomes, whereas another kainate receptor subunit (KA2), the *N*-methyl-D-aspartic acid receptor subunits (NR1, NR2A, NR2B), the AMPA receptor subunits (GluR1, GluR2), actinfilin, and actin levels remain relatively unchanged.

Levels of polyubiquitinated GluR6 were also determined by pulldown experiments utilizing the high-affinity polyubiquitin binding proteasome subunit S5a conjugated to GST-agarose beads (22). To compare the relative levels of GluR6 ubiquitination, we equalized synaptic GluR6 levels from the wild-type and heterozygous $Cul3^{+/-}$ mice, and then performed pull-down experiments. More ubiquitinated GluR6 was found in wild-type mice as compared with mice heterozygous for *Cul3* (Fig. 6*C*). These results are consistent with Cul3 playing a role in regulating GluR6 levels at the synapse and further implicates Cul3 as a mediator in GluR6 ubiquitination.

Actinfilin and Cul3 Negatively Regulate Surface GluR6 in Hippocampal Neurons—To determine how actinfilin affects the localization of GluR6 in neurons, we expressed a small inhibitory RNA to actinfilin (RNAi-AF) or the dominant-negative *CUL3* construct (Fig. 7). The surface levels and subcellular localization of both endogenous GluR6 and transfected GFP-tagged GluR6 were determined immunocytochemically. Potential regulation of synaptic localization was assessed by co-staining for synaptic markers (PSD-95 and synaptophysin).

[3] J. D. Gonzales and J. D. Singer, submitted for publication.

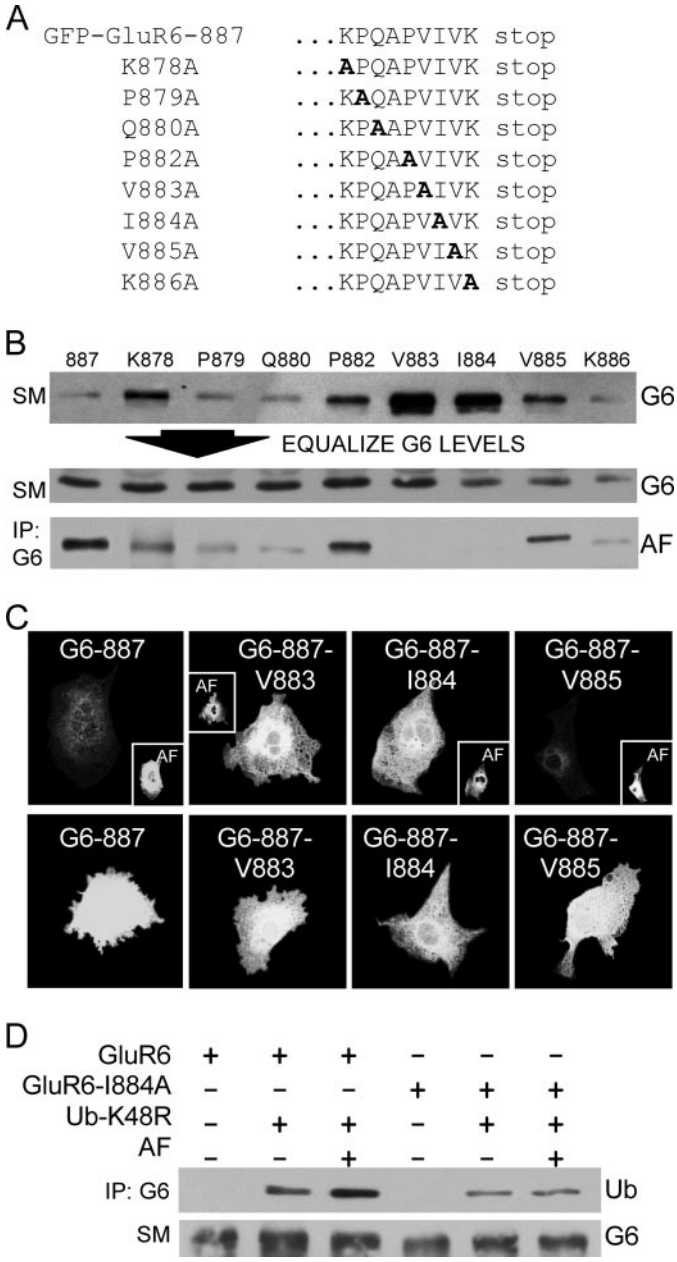

FIGURE 5. **A hydrophobic amino acid region near the GluR6 C terminus is critical for actinfilin binding.** *A*, schematic of point mutations made in the GFP-G6–887 construct. GluR6–887 was used here because its interaction with AF is more easily detectable because less is degraded (see Fig. 4*B*). *B*, to map the residue(s) critical for actinfilin binding, the alanine substitution constructs shown in *A* were expressed in HEK293 cells and their ability to co-immunoprecipitate with myc-tagged AF was tested. Because we found that these constructs had varying expression levels (*top*), the GluR6 levels (*G6*) were equalized (*middle*) to determine proper ratios for AF co-immunoprecipitation (*bottom*: *IP*, *G6*, then immunoprobed for AF). For reference, the first lane shows the total level of wild-type GluR6–887 expression (*top*) and the amount that co-precipitates with AF (*bottom*). We found that the V883A and I884A mutants had increased expression as well as decreased AF binding. *C*, the V883A and I884A mutations protect GFP-G6–887 from AF-mediated degradation. COS7 cells were transfected as indicated, permeabilized, and stained with antibodies against GFP (*main panels*) or myc-AF (*insets*). *Top panels*, when co-expressed with AF, G6–887-V883A and -I884A levels are high, but wild-type G6–887 and G6–887-V885 levels are low, presumably due to AF-induced degradation. *Bottom panels*, controls showing that in the absence of exogenous AF, all G6 constructs are easily detectable. *D*, actinfilin acts as an adaptor, linking GluR6 to the ubiquitin-proteasome pathway. GFP-tagged wild-type GluR6 or GluR6-I884A were cotransfected with HA-tagged ubiquitin-K48R and/or myc-tagged AF into HEK293 cells. To block loss of receptors via proteasomal degradation, cells were treated with 10 μM MG132 10 h prior to solubilization. GluR6 was immunoprecipitated from cell extracts with anti-GFP antibodies, and immunoblotted for HA to determine the levels of ubiquitinated receptor. *Upper blot*, in the absence of AF and the Ub-K48R construct that blocks polyubiquination, no ubiquitination of GluR6 can be detected (*lanes 1* and *4*). However, in the presence of Ub-K48R, AF increases wild-type GluR6 ubiquitination (*lanes 2 versus 3*), but fails to increase ubiquitination of the I884A mutant (*lanes 5 versus 6*). *Lower blot*, equal levels of immunoprecipitated receptor in the SM are shown by immunoprobing for GFP.

We found that decreasing actinfilin levels via RNAi significantly increased surface GluR6 expression in dendritic spines, as assessed morphologically and by increased co-localization with PSD-95 (Fig. 7, *A–D* and *H*) and synaptophysin (Fig. 7*H*). Synaptic GluR6 more than doubled (Fig. 7*H*), and the size of the GluR6-containing puncta increased 1.8-fold (mean punctal area ± S.E.: control neurons, 0.12 ± 0.01 μm^2; RNAi-AF expressing neurons, 0.22 ± 0.01 μm^2). That the RNAi-AF was effective in reducing actinfilin levels is demonstrated in Fig. 7, *E* and *F*; importantly, however, the low remaining actinfilin retained a normal subcellular distribution (see also Fig. 7*H*, *far right bars*). Interestingly, in the absence of RNAi knock-down of actinfilin, relatively little GluR6 was detected in the spines and co-localization with synaptic markers was low (Fig. 7, *A–D* and *H*). Overexpression of the dominant-negative Cul3 produced similar effects (Fig. 7, *G* and *H*). Together, our results suggest that actinfilin-Cul3-mediated degradation may provide an important mechanism for regulating neuronal GluR6 surface expression and, in particular, for regulating GluR6 levels at synapses.

DISCUSSION

At synapses there is increasing evidence for the role of ubiquitination in regulating the number of glutamate receptors and scaffold and signaling proteins (20–22, 34, 35). In *Caenorhabditis elegans*, ubiquitination of the glutamate receptor subunit GLR-1 regulates endocytosis, and the BTB-Kelch protein KEL-8-Cul3 complex is required for ubiquitin-mediated GLR-1 turnover (34, 36). At mammalian synapses, an F-box protein, Fbx2, promotes ubiquitination of the *N*-methyl-D-aspartic acid receptor NR1 subunit, inducing retrotranslocation and degradation by the ubiquitin-proteasome pathway (37).

Here, we provide evidence that actinfilin, a brain-enriched BTB-Kelch protein, acts as a scaffold linking the kainate receptor subunit GluR6 to the Cullin 3 ubiquitin-ligase (Cul3). Actinfilin is localized, but not limited, to the dendritic spine, a structure rich in actin and critical for synapse formation (26, 38). We find that actinfilin controls both the synaptic localization and the size of synaptic GluR6-containing kainate receptor clusters in primary hippocampal neurons. In the presence of normal levels of actinfilin, detectable synaptic GluR6 was relatively low (~20%). However, down-regulating actinfilin via a specific RNAi increased both the synaptic localization and the size of synaptic GluR6-containing kainate receptor clusters, as did expression of a dominant-negative Cul3. Recent studies demonstrate that ubiquitination can modulate AChR assembly efficiency to control the number of mature receptors on the plasma membrane (39). Similarly, actinfilin could function to regulate assembly of kainate receptors by targeting receptor subunit ubiquitination as part of the endoplasmic reticulum-

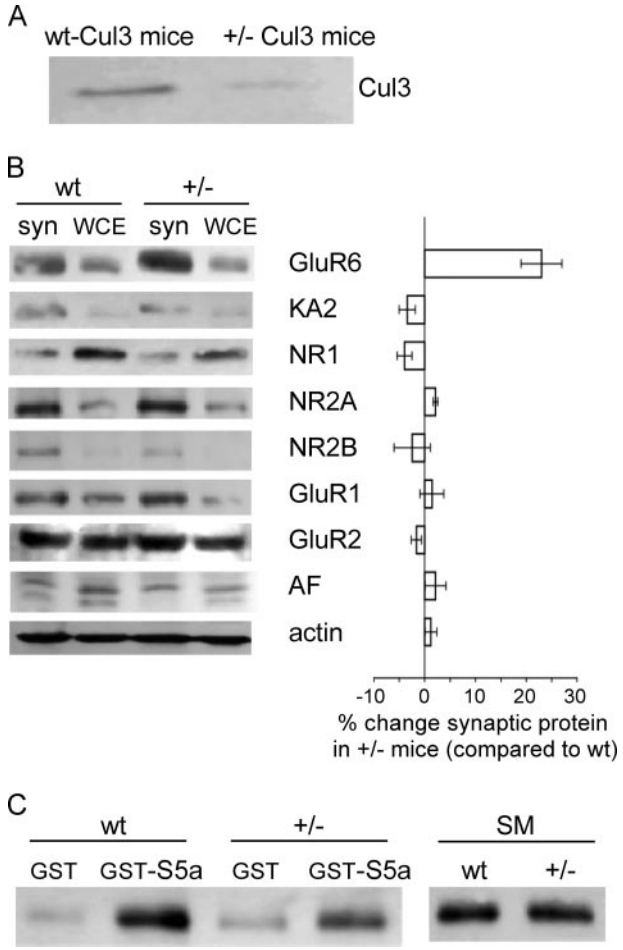

FIGURE 6. **Cul3 regulates GluR6 expression *in vivo*.** *A*, mice heterozygous for Cul3 have lowered neuronal *Cul3* levels. Total brain extracts of P14 *Cul3* wild-type and +/− heterozygous mice (see "Experimental Procedures") were immunoprobed for the presence of Cul3. *B*, reducing Cul3 increases synaptic GluR6 levels. Equal amounts of synaptosomal fractions (*syn*) and whole cell extracts (*WCE*) from wild-type (*wt*) and *Cul3* heterozygous (+/−) mice were resolved by SDS-PAGE to determine protein levels. To calculate the percentage change of synaptic proteins, densitometry was performed and the levels in synaptosomes obtained from heterozygous mice were compared with the wild-type amounts. In heterozygous $Cul3^{+/-}$ mice, GluR6 levels dramatically increased (23.0 ± 4.0%; mean ± S.E.), whereas the levels of KA2 (−3.4 ± 1.6%), NR1 (4.0 ± 1.5%), NR2A (2.2 ± 0.5%), NR2B (−2.5 ± 3.6), GluR1 (1.5 ± 2.4%), GluR2 (−1.6 ± 1.0%), actinfilin (2.2 ± 2.0%), and actin (1.2 ± 1.1%) remained approximately the same. $n = 3$ independent experiments. *C*, GluR6 ubiquitination is reduced in $Cul3^{+/-}$ mice. Western blots of synaptosomes were first probed for GluR6 to determine GluR6 levels in $Cul3^{+/-}$ and $Cul3^{+/+}$ mice. Ubiquitinated synaptosomal proteins were then pulled down using GST-agarose (control) or GST-5a-agarose (ubiquitinated proteins) as described under "Experimental Procedures." The pull-down products were loaded onto SDS-PAGE gels in a ratio that equalized the GluR6 levels in $Cul3^{+/-}$ and $Cul3^{+/+}$ synaptosomes, and probed for GluR6 to establish the levels of ubiquitinated receptor. As shown here, GluR6 has higher levels of ubiquitination in wild-type mice (*wt*) than heterozygous *Cul3* mice (+/−), because lowered Cul3 expression inhibits its proper ubiquitination. *Right panel*, control Western blot showing that equal amounts of GluR6 were present in the wild-type and +/− SM used for the pull-downs.

associated degradation pathway (40). Alternatively, it is also possible that ubiquitination is needed for kainate receptor endocytosis. The synaptic localization of actinfilin suggests a role in regulating the ubiquitination of synaptic surface kainate receptors or scaffold proteins involved in trafficking. Although ubiquitination is known to regulate the internalization of some surface receptors, such as the β_2-adrenergic and epidermal growth factor receptors for lysosomal degradation (41, 42), proteasomal degradation of mature surface receptors would necessitate a mechanism for retrotranslocation. Nevertheless, the degradation of synaptic NR1 subunits has recently been proposed to involve relocation to the dendrites and soma for retrotranslocation and proteasomal degradation (37).

We propose that actinfilin contains two functional domains that mediate degradation: a BTB domain that binds Cul3-based ligases and a Kelch domain that interacts with the substrate (see model, Fig. 3*E*). This model is based on the well characterized Skp1-Cul1-F-box protein complex in which the Cul1-interacting domain of Skp1 forms a BTB structure (24). However, in the yeast two-hybrid system, we find that deleting the BTB domain and the majority of the BACK domain, a region that links the BTB and Kelch domains, appears to decrease GluR6-Kelch interaction. Because the BACK domain has been suggested to be involved in substrate orientation, removal of this region may limit the ability of the Kelch repeat to interact with GluR6 (43). Alternatively, the actinfilin BTB domain may serve as a dimerization domain needed for effective substrate binding (44).

The function of actinfilin in ubiquitination is consistent with recent studies showing that several BTB-containing proteins can function as Cul3 adaptors (24, 31, 33, 45, 46). KLHL12, which shows 40% amino acid identity to actinfilin, acts as a Cul3 adaptor, targeting Dishevelled for degradation (47), as does Keap1 (35% identity), which targets the transcriptional activator Nrf2 (30–32, 46). Gigaxonin, which shows little homology to actinfilin (23%) and is mutated in human giant axonal neuropathy has recently been found to ubiquitinate and subsequently degrade tubulin folding cofactor B (48). In contrast, the actin-binding BTB-Kelch proteins, KLHL20 (KLEIP) and Mayven (Kelch-like 2), which show the highest similarity to actinfilin, so far have not been implicated in ubiquitination (49, 50). Additionally, there are a number of BTB-Kelch proteins that exhibit a high degree of similarity to actinfilin but have unknown functions. It remains to be determined how many of these will act as substrate adaptors for Cul3 ubiquitin ligases.

We also find that removing the last four amino acids from the GluR6 C terminus results in loss of actinfilin binding. This suggests that the C terminus, which contains a type I PDZ-binding motif (ETMA), adopts a specific structure. Interestingly, this motif associates with various PDZ-containing scaffolding proteins, such as PSD-95 or SAP97, and is required for proper clustering of GluR6-containing kainate receptors within the synapse (7). Once these residues are deleted, the C-terminal tail of the GluR6 protein may fold back on itself to prevent binding to actinfilin. In contrast, full-length GluR6 may interact with endogenously expressed PDZ domain scaffolding proteins to facilitate actinfilin binding (7, 10). Intriguingly, actinfilin-GluR6 binding is restored after removal of an additional 17 residues up to a 5-amino acid "hydrophobic" site (APVIV); deletion or substitution of the hydrophobic residues again results in loss of actinfilin-GluR6 binding. However, this site is not conserved in GluR5, which we showed can also bind actinfilin. This suggests that although the hydrophobic site is a determinant of actinfilin binding, it may not encompass the binding site. Instead, it may affect the C-terminal structure, possibly through an interaction of this domain with the mem-

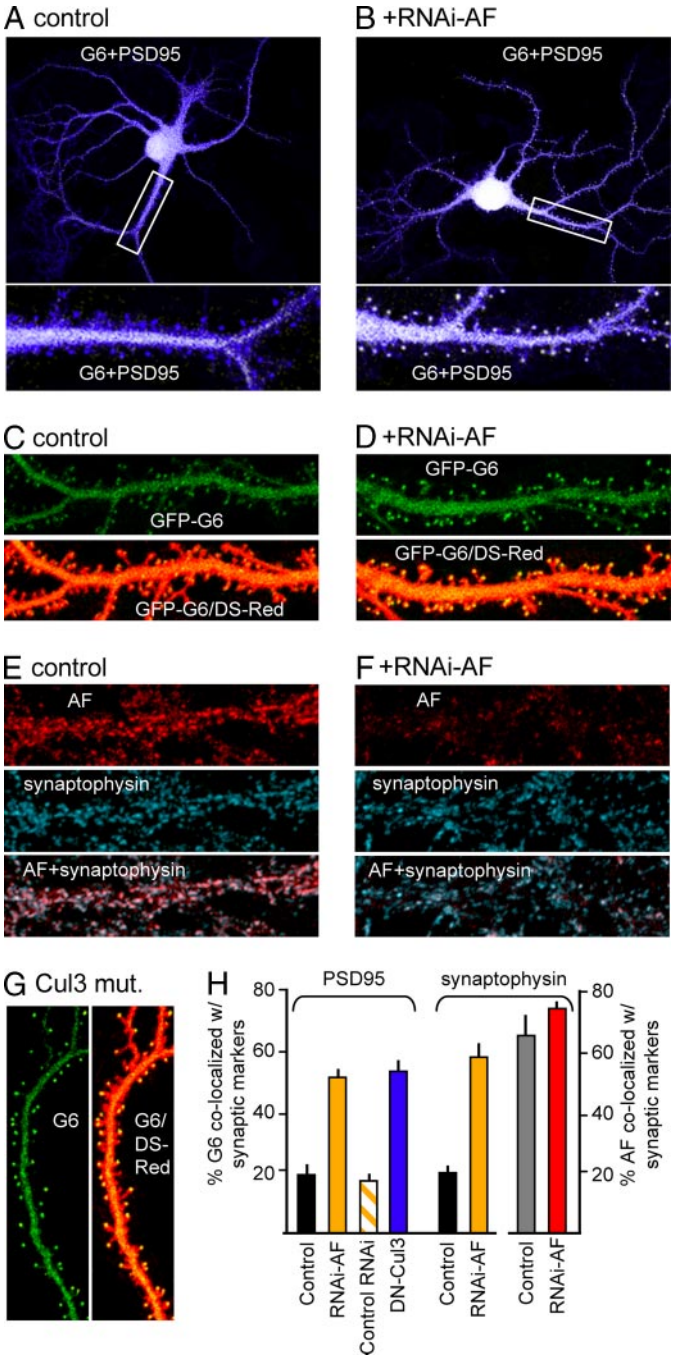

FIGURE 7. **Actinfilin and Cul3 negatively regulate surface expression of GluR6.** *A* and *B*, compared with control hippocampal neurons (*A*), reducing AF levels with a small inhibitory RNA (RNAi-AF) increases GluR6 (G6) surface levels (*B*). Surface expression of endogenous GluR6 was detected by indirect immunofluorescence using an antibody against an extracellular GluR6 epitope and a Cy5-conjugated secondary antibody (see "Experimental Procedures"). Neurons were also transfected with yellow fluorescent protein-tagged PSD-95 to identify synapses. Shown here are superimposed images of YFP-PSD-95 (*blue*) and surface G6 (*yellow*), with areas of co-localization appearing almost white and areas with relatively little G6 (*e.g.* the synaptic spine heads in *A*) appearing *deep blue*. The *lower images*, indicated by the *white boxes* on the *upper frames*, demonstrate that decreasing AF results in increased surface G6 in dendritic shafts and synaptic spines (*B*). *C* and *D*, similar results are obtained when hippocampal neurons were transfected with GluR6 tagged extracellularly with GFP and, to identify cellular morphology, DS-Red. Again, compared with control neurons (*C*), reducing AF levels with RNAi-AF increases G6 surface levels (*D*). *Upper panels* demonstrate the surface expression of the GFP-G6. To clarify the locations of dendritic spines and underscore the RNAi-AF-induced increase of surface G6 in spine heads (*D*), the *lower panels* are superimposed images of GFP-G6 and DS-Red; here, *yellow* indicates where G6 levels are elevated. *E* and *F*, RNAi-AF strongly reduces AF levels in hippocampal neurons without altering the distribution of any remaining AF (see also *H*). *G*, overexpressing the dominant negative Cul3 mutant also results in high surface levels of endogenous G6 (indirect immunofluorescence using a fluorescein isothiocyanate-conjugated secondary antibody). Co-transfection with DS-Red was used to establish neuronal morphology; the *right panel* emphasizes the prominent surface expression of G6 in most spine heads (*i.e.* most but not all spine heads are *yellow* due to the strong fluorescein isothiocyanate signal in the G6 and DS-Red overlay). *H*, reducing AF increases G6 co-localization with synaptic markers. Surface expression of endogenous G6 was detected as in *A*, *B*, and *G*, and the % co-localization with YFP-PSD-95 or synaptophysin determined. Each *bar* indicates the mean ± S.E. for the specified condition. The *far right pair of bars* demonstrates that, even though the RNAi-AF effectively reduces AF levels (see *E* and *F*), the low remaining AF retains a normal cellular distribution with regard to synaptic markers.

brane. The site is immediately distal to a forward trafficking domain located between residues 871 and 877 (CQRRLKH) that includes cysteine 871, one of two such residues in the GluR6 C terminus known to be palmitoylated (51). Moreover, hydrophobic residues occur at an unusually high frequency near the palmitoylated cysteines and substitution of any of these residues with alanine reduces palmitoylation (52, 53). Thus, the hydrophobic site could function in GluR6 palmitoylation to stabilize the C terminus in a conformation capable of actinfilin binding.

Our results indicate that in heterologous cells actinfilin is ubiquitinated and that its protein levels are regulated by Cul3. Overexpression of wild-type Cul3 lowers actinfilin levels, whereas transfection of a mutant L52A/E55A Cul3 or Cul1 has no such effect, suggesting that actinfilin might be co-degraded with its substrate. Similarly, Keap1 and several F-box and SOCS adaptor proteins appear to be degraded by autocatalytic mechanisms, although Keap1 degradation occurs in a proteasome-independent manner (46). Here, we observed modest effects of lysosomal inhibition on actinfilin levels in heterologous cells. We also found, however, that actinfilin levels did not significantly increase in *Cul3*$^{+/-}$ mice, suggesting that lysosomal degradation may provide a second means for regulating actinfilin; additionally, the fact that Cul3 is only reduced but not eliminated may be a contributing factor. We further observed that KA2 levels did not change in the *Cul3* heterozygous mice. Because our work and others have shown that GluR6 knock-out results in the reduced KA2 due to endoplasmic reticulum retention signals that prevent surface expression of KA2 in the absence of GluR5-GluR7 subunits (3, 4, 54), the absence of regulation of KA2 levels in the *Cul3*$^{+/-}$ mice raises the possibility that *in vivo* actinfilin may preferentially promote the proteasomal degradation of homomeric receptors.

Actinfilin and other BTB-Kelch proteins, such as Keap1, have been shown to associate with the actin cytoskeleton, and interactions with actin are necessary for Keap1 to regulate levels of Nrf2 (55). Interestingly, synaptic activity is known to promote the redistribution of proteasomes from dendritic shafts to spines via an association with actin filaments (21). Similarly, the actin cytoskeleton and/or other scaffolding proteins may regulate actinfilin function. One potential regulator may be cystic fibrosis transmembrane regulator-associated protein 70, CAP70, a scaffold protein with four PDZ domains. Chen and Li (27, 56) have recently shown that CAP70 binds to the actinfilin C-terminal

PDZ-binding motif. CAP70 is also associated with the post-synaptic density proteins PSD-95, synaptic RasGAP (synGAP), and GKAP, suggesting possible roles for these proteins in regulating kainate receptor-actinfilin binding or the trafficking of actinfilin-bound GluR6 to the degradation machinery.

Studies *in vivo* demonstrate that postsynaptic kainate receptors can perform multiple functions; a metabotropic role and, in restricted neuronal populations, the generation of kainate receptor-mediated excitatory post-synaptic currents (1, 2). Because GluR6 has been implicated in excitotoxic neuronal death via activation of a mixed-lineage kinase and c-Jun N-terminal kinase (57), and in particular with damage associated with cerebral ischemia, stroke, and epileptic seizures, our data imply that actinfilin may provide an important means for ensuring the correct regulation of GluR6 surface expression. In addition, recent studies have utilized peptides to inhibit GluR6 clustering to protect neurons from kainate receptor-mediated cell death (58, 59), and suggest that actinfilin may prove to be a useful therapeutic target to control endogenous synaptic GluR6.

Acknowledgments—We thank Nathan Riley who assisted in the early stages of this project and Dr. Dale Mierke in identifying the GluR6 antigenic site that was used to generate the GluR6 antibody. We also thank Fernanda Laezza and Ann Marie Craig for useful discussions of Kelch proteins.

REFERENCES

1. Lerma, J. (2006) *Curr. Opin. Pharmacol.* **6,** 89–97
2. Pinheiro, P., and Mulle, C. (2006) *Cell Tissue Res.* **326,** 457–482
3. Nasu-Nishimura, Y., Hurtado, D., Braud, S., Tang, T. T., Isaac, J. T., and Roche, K. W. (2006) *J. Neurosci.* **26,** 7014–7021
4. Ren, Z., Riley, N. J., Garcia, E. P., Sanders, J. M., Swanson, G. T., and Marshall, J. (2003) *J. Neurosci.* **23,** 6608–6616
5. Ren, Z., Riley, N. J., Needleman, L. A., Sanders, J. M., Swanson, G. T., and Marshall, J. (2003) *J. Biol. Chem.* **278,** 52700–52709
6. Ruiz, A., Sachidhanandam, S., Utvik, J. K., Coussen, F., and Mulle, C. (2005) *J. Neurosci.* **25,** 11710–11718
7. Garcia, E. P., Mehta, S., Blair, L. A. C., Wells, D. G., Shang, J., Fukushima, T., Fallon, J. R., Garner, C. C., and Marshall, J. (1998) *Neuron* **21,** 727–739
8. Hirbec, H., Francis, J. C., Lauri, S. E., Braithwaite, S. P., Coussen, F., Mulle, C., Dev, K. K., Coutinho, V., Meyer, G., Isaac, J. T., Collingridge, G. L., and Henley, J. M. (2003) *Neuron* **37,** 625–638
9. Jaskolski, F., Coussen, F., Nagarajan, N., Normand, E., Rosenmund, C., and Mulle, C. (2004) *J. Neurosci.* **24,** 2506–2515
10. Mehta, S., Wu, H., Garner, C. C., and Marshall, J. (2001) *J. Biol. Chem.* **276,** 16092–16099
11. Yan, S., Sanders, J. M., Xu, J., Zhu, Y., Contractor, A., and Swanson, G. T. (2004) *J. Neurosci.* **24,** 679–691
12. Castillo, P. E., Malenka, R. C., and Nicoll, R. A. (1997) *Nature* **388,** 182–186
13. Contractor, A., Swanson, G., and Heinemann, S. F. (2001) *Neuron* **29,** 209–216
14. Mulle, C., Sailer, A., Perez-Otano, I., Dickinson-Anson, H., Castillo, P. E., Bureau, I., Maron, C., Gage, F. H., Mann, J. R., Bettler, B., and Heinemann, S. F. (1998) *Nature* **392,** 601–605
15. Vignes, M., and Collingridge, G. L. (1997) *Nature* **388,** 179–182
16. Fisahn, A., Contractor, A., Traub, R. D., Buhl, E. H., Heinemann, S. F., and McBain, C. J. (2004) *J. Neurosci.* **24,** 9658–9668
17. Fisahn, A., Heinemann, S. F., and McBain, C. J. (2005) *J. Physiol.* **562,** 199–203
18. Melyan, Z., Lancaster, B., and Wheal, H. V. (2004) *J. Neurosci.* **24,** 4530–4534
19. Martin, S., and Henley, J. M. (2004) *EMBO J.* **23,** 4749–4759
20. Pak, D. T., and Sheng, M. (2003) *Science* **302,** 1368–1373
21. Bingol, B., and Schuman, E. M. (2006) *Nature* **441,** 1144–1148
22. Ehlers, M. D. (2003) *Nat. Neurosci.* **6,** 231–242
23. Petroski, M. D., and Deshaies, R. J. (2005) *Nat. Rev. Mol. Cell. Biol.* **6,** 9–20
24. Pintard, L., Willems, A., and Peter, M. (2004) *EMBO J.* **23,** 1681–1687
25. van den Heuvel, S. (2004) *Curr. Biol.* **14,** R59–R61
26. Chen, Y., Derin, R., Petralia, R. S., and Li, M. (2002) *J. Biol. Chem.* **277,** 30495–30501
27. Chen, Y., and Li, M. (2005) *Neuropharmacology* **49,** 1026–1041
28. Goslin, K., and Banker, G. (1989) *J. Cell Biol.* **108,** 1507–1516
29. Singer, J. D., Gurian-West, M., Clurman, B., and Roberts, J. M. (1999) *Genes Dev.* **13,** 2375–2387
30. Cullinan, S. B., Gordan, J. D., Jin, J., Harper, J. W., and Diehl, J. A. (2004) *Mol. Cell. Biol.* **24,** 8477–8486
31. Furukawa, M., and Xiong, Y. (2005) *Mol. Cell. Biol.* **25,** 162–171
32. Kobayashi, A., Kang, M. I., Okawa, H., Ohtsuji, M., Zenke, Y., Chiba, T., Igarashi, K., and Yamamoto, M. (2004) *Mol. Cell. Biol.* **24,** 7130–7139
33. Xu, L., Wei, Y., Reboul, J., Vaglio, P., Shin, T. H., Vidal, M., Elledge, S. J., and Harper, J. W. (2003) *Nature* **425,** 316–321
34. Burbea, M., Dreier, L., Dittman, J. S., Grunwald, M. E., and Kaplan, J. M. (2002) *Neuron* **35,** 107–120
35. Hegde, A. N., and DiAntonio, A. (2002) *Nat. Rev. Neurosci.* **3,** 854–861
36. Schaefer, H., and Rongo, C. (2006) *Mol. Biol. Cell* **17,** 1250–1260
37. Kato, A., Rouach, N., Nicoll, R. A., and Bredt, D. S. (2005) *Proc. Natl. Acad. Sci. U. S. A.* **102,** 5600–5605
38. Allison, D. W., Gelfand, V. I., Spector, I., and Craig, A. M. (1998) *J. Neurosci.* **18,** 2423–2436
39. Christianson, J. C., and Green, W. N. (2004) *EMBO J.* **23,** 4156–4165
40. Brodsky, J. L., and McCracken, A. A. (1999) *Semin. Cell. Dev. Biol.* **10,** 507–513
41. Huang, F., Kirkpatrick, D., Jiang, X., Gygi, S., and Sorkin, A. (2006) *Mol. Cell* **21,** 737–748
42. Shenoy, S. K., McDonald, P. H., Kohout, T. A., and Lefkowitz, R. J. (2001) *Science* **294,** 1307–1313
43. Stogios, P. J., and Prive, G. G. (2004) *Trends Biochem. Sci.* **29,** 634–637
44. McMahon, M. J., Thomas, N., Itoh, K., Yamamoto, M., and Hayes, J. D. (2006) *J. Biol. Chem.* **281,** 24756–24768
45. Geyer, R., Wee, S., Anderson, S., Yates, J., and Wolf, D. A. (2003) *Mol. Cell* **12,** 783–790
46. Zhang, D. D., Lo, S. C., Sun, Z., Habib, G. M., Lieberman, M. W., and Hannink, M. (2005) *J. Biol. Chem.* **280,** 30091–30099
47. Angers, S., Thorpe, C. J., Biechele, T. L., Goldenberg, S. J., Zheng, N., MacCoss, M. J., and Moon, R. T. (2006) *Nat. Cell. Biol.* **8,** 348–357
48. Wang, W., Ding, J., Allen, E., Zhu, P., Zhang, L., Vogel, H., and Yang, Y. (2005) *Curr. Biol.* **15,** 2050–2055
49. Hara, T., Ishida, H., Raziuddin, R., Dorkhom, S., Kamijo, K., and Miki, T. (2004) *Mol. Biol. Cell* **15,** 1172–1184
50. Jiang, S., Avraham, H. K., Park, S. Y., Kim, T. A., Bu, X., Seng, S., and Avraham, S. (2005) *J. Neurochem.* **92,** 1191–1203
51. Pickering, D. S., Taverna, F. A., Salter, M. W., and Hampson, D. R. (1995) *Proc. Natl. Acad. Sci. U. S. A.* **92,** 12090–12094
52. Belanger, C., Ansanay, H., Qanbar, R., and Bouvier, M. (2001) *FEBS Lett.* **499,** 59–64
53. ten Brinke, A., Vaandrager, A. B., Haagsman, H. P., Ridder, A. N., van Golde, L. M., and Batenburg, J. J. (2002) *Biochem. J.* **361,** 663–671
54. Christensen, J. K., Paternain, A. V., Selak, S., Ahring, P. K., and Lerma, J. (2004) *J. Neurosci.* **24,** 8986–8993
55. Kang, M. I., Kobayashi, A., Wakabayashi, N., Kim, S. G., and Yamamoto, M. (2004) *Proc. Natl. Acad. Sci. U. S. A.* **101,** 2046–2051
56. Wang, S., Yue, H., Derin, R. B., Guggino, W. B., and Li, M. (2000) *Cell* **103,** 169–179
57. Savinainen, A., Garcia, E. P., Dorow, D., Marshall, J., and Liu, Y. F. (2001) *J. Biol. Chem.* **276,** 11382–11386
58. Liu, X. M., Pei, D. S., Guan, Q. H., Sun, Y. F., Wang, X. T., Zhang, Q. X., and Zhang, G. Y. (2006) *J. Biol. Chem.* **281,** 17432–17445
59. Piserchio, A., Salinas, G. D., Li, T., Marshall, J., Spaller, M. R., and Mierke, D. F. (2004) *Chem. Biol.* **11,** 469–473